INTERFACE

royalsocietypublishing.org/journal/rsif

Research

Cite this article: Jorge JF, Patek SN. 2023 Elastic pinch biomechanisms can yield consistent launch speeds regardless of projectile mass. *J. R. Soc. Interface* **20**: 20230234.
https://doi.org/10.1098/rsif.2023.0234

Received: 20 April 2023
Accepted: 26 July 2023

Subject Category:
Life Sciences–Physics interface

Subject Areas:
biomechanics, biophysics, biomaterials

Keywords:
ballistochory, spring actuation, elastic potential energy, kinematics, plant biomechanics, scaling

Author for correspondence:
Justin F. Jorge
e-mail: justinfjorge@gmail.com

Electronic supplementary material is available online at https://doi.org/10.6084/m9.figshare.c.6777699.

THE ROYAL SOCIETY PUBLISHING

Elastic pinch biomechanisms can yield consistent launch speeds regardless of projectile mass

Justin F. Jorge and S. N. Patek

Department of Biology, Duke University, Durham, NC, USA

JFJ, 0000-0002-7030-0610; SNP, 0000-0001-9738-882X

Energetic trade-offs are particularly pertinent to bio-ballistic systems which impart energy to projectiles exclusively during launch. We investigated such trade-offs in the spring-propelled seeds of *Loropetalum chinense*, *Hamamelis virginiana* and *Fortunearia sinensis*. Using similar seed-shooting mechanisms, fruits of these confamilial plants (Hamamelidaceae) span an order of magnitude in spring and seed mass. We expected that as seed mass increases, launch speed decreases. Instead, launch speed was relatively constant regardless of seed mass. We tested if fruits shoot larger seeds by storing more elastic potential energy (PE). Spring mass and PE increased as seed mass increased (in order of increasing seed mass: *L. chinense*, *H. virginiana*, *F. sinensis*). As seed mass to spring mass ratio increased (ratios: *H. virginiana* = 0.50, *F. sinensis* = 0.65, *L. chinense* = 0.84), mass-specific PE storage increased. The conversion efficiency of PE to seed kinetic energy (KE) decreased with increasing fruit mass. Therefore, similar launch speeds across scales occurred because (i) larger fruits stored more PE and (ii) smaller fruits had higher mass-specific PE storage and improved PE to KE conversion. By examining integrated spring and projectile mechanics in our focal species, we revealed diverse, energetic scaling strategies relevant to spring-propelled systems navigating energetic trade-offs.

1. Introduction

The fastest motions in biology consist of lightweight projectiles that are accelerated by springs [1–11]. Across kingdoms, examples of biological springs include the bow-shaped exoskeletal structures on the legs of froghoppers [1], the everting membrane of the cannonball fungus [8] and the buckling walls of carnivorous bladderwort plant traps [12]. Equally diverse are the projectiles launched by these springs such as the entire body of the froghopper, a mass of spores and the walls of the trap for the previous examples, respectively. These diverse mechanisms, which span kingdoms, functions and size scales, operate within the mechanical principles of spring recoil and projectile dynamics [8,13–15]. We investigated the relationship between springs and projectiles through the seed-shooting witch hazel study system.

Spring actuation is defined as the transformation of elastic potential energy stored in the spring into kinetic energy of the projectile. Therefore, given a constant amount of energy in the spring, there is a tradeoff between the mass of the projectile and its launch speed [13]. This is exemplified by the decreasing speeds of progressively heavier arrows shot by a crossbow [16]. Similarly, the launch speeds of appendages, mandibles, propagules, or other spring-launched biological projectiles are expected to decrease as they increase in mass if the elastic potential energy is held constant [13]. Biological examples include multifunctional systems in which the spring-launched projectile varies across functions. Trap-jaw ants can launch their 145 µg mandibles against prey at speeds up to 60 m s^{-1} or use the same mandible strike against the ground to propel their entire 15 mg body at much slower speeds of 0.24 m s^{-1} [6]. Similarly, a grasshopper can use its legs to kick away predators, moving its 21 mg tibia at around

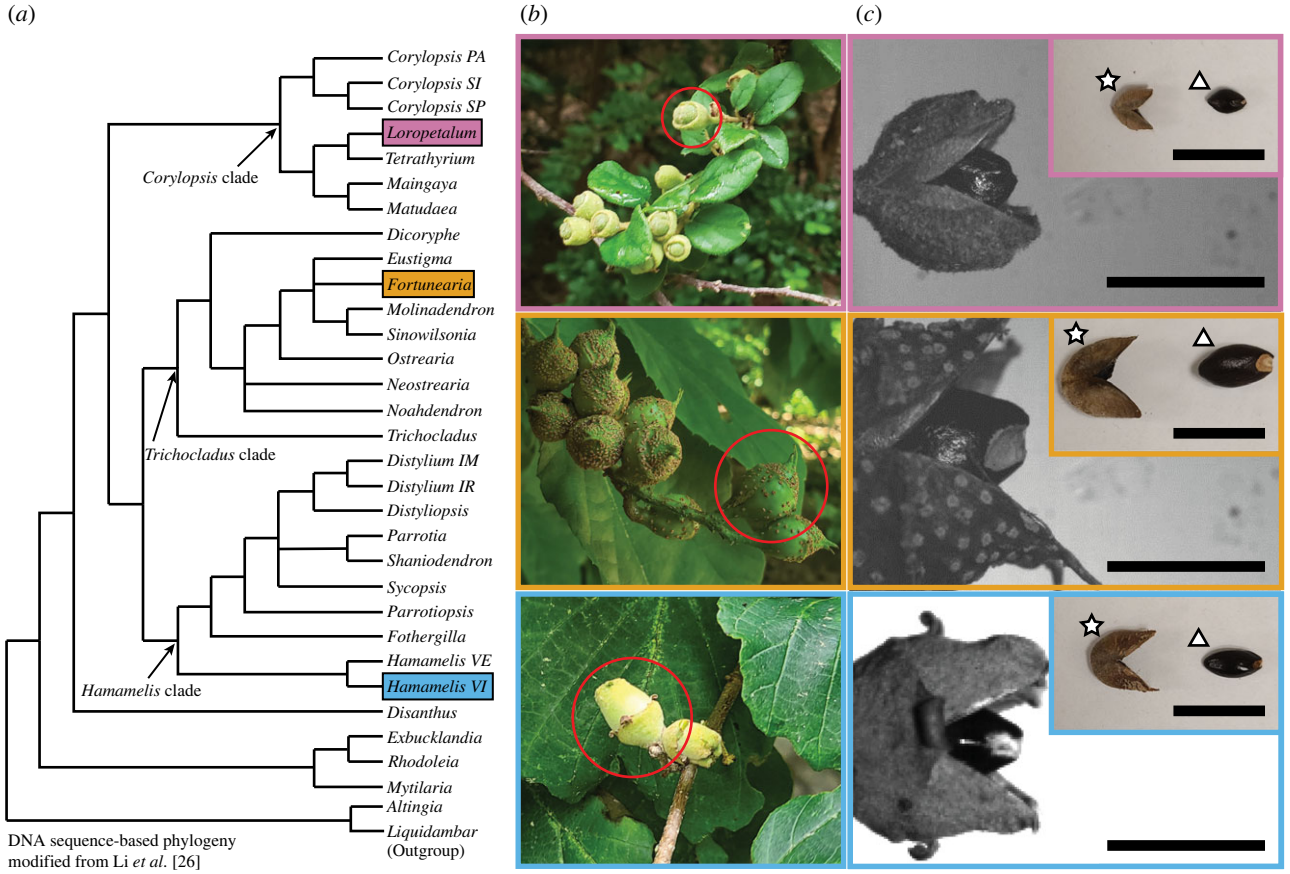

Figure 1. The three focal species are diverse in size and structure yet share a pinch-based seed-shooting mechanism. (*a*) The three focal species, *Loropetalum chinense*, *Fortunearia sinensis* and *Hamamelis virginiana* (*Hamamelis VI* and *Hamamelis VE* refer to *H. virginiana* and *H. vernalis*, respectively), represent seed-shooting plants from each of the major Hamamelidaceae clades. (*b*) The external structure of the fruits, as well as the plants from which they grow, vary across the three species. A single fruit is circled in red in each picture. The fruits in these images are not yet mature. (*c*) Mature fruits split open revealing one to two seeds. Each seed is launched by its own endocarp. As displayed in the insets, when the outer layer of the fruit (referred to as the exocarp) is peeled away, a similar looking endocarp (star) and seed (triangle) are observed across species. Note that only one of the two pairs of endocarps and their accompanying seeds is shown in the insets. Scale bars indicate 1 cm.

80° ms^{-1} (linear speed of up to 28 m s^{-1} for a 20 mm long tibia), or use the same system to launch its 3 g body at 3 m s^{-1} [17,18].

However, elastic potential energy need not be held constant for spring-propelled projectiles. Returning to the crossbow example, a crossbow can shoot heavier arrows at similar or even greater speeds than lighter arrows if the bowstring is drawn back further for the heavier arrows or if a different crossbow is used that requires more force or displacement and can thereby store more elastic potential energy. Variation in elastic potential energy storage across biological springs is expected when comparing springs across kingdoms which vary in size, shape and material composition [8]. Even across the scaling of related biological systems, elastic potential energy storage varies. For example, elastic potential energy storage in the tendons of jumping marsupials increases with increasing body mass [19]. Furthermore, across individuals of the same species of mantis shrimp, *Gonodactylaceus falcatus*, elastic potential energy storage increased with body mass [20].

Diverse plants use spring actuation to launch seeds out of fruits [21]. In flowering plants, the fruit is a specialized structure with the primary function of aiding in the dispersal of seeds or other propagules [22]. Plants with seed-shooting fruits disperse their seeds by launching them with springs [8]. Generally, the mechanism of seed launch is as follows: the slow transport of water in or out of cells deforms a spring within the fruit that later rapidly recoils to launch one or many seeds [15]. The basic building blocks of spring propulsion in flowering plants span considerable sizes. Spring mass spans at least three orders of magnitude (0.1 mg range for springs of *Oxalis* spp. to the 100 mg range for springs of *Fortunearia sinensis* [23]) while seed mass spans at least four orders of magnitude (0.1 mg seeds of *Cardamine hirsuta* to the 1 g seeds of *Hura crepitans* [11,24,25]).

Within the flowering plants are seed-shooting species of the witch hazel family (Hamamelidaceae) which are particularly well suited for studying the energetics of springs and seeds across scales. Among the seed-shooting Hamamelidaceae species, we selected *Loropetalum chinense*, *Hamamelis virginiana* and *Fortunearia sinensis* as our focal species [26]. The fruits of these species shoot their seeds with a pinch mechanism [26–28], yet their springs and seeds span an order of magnitude in mass (ranging from 20 mg to 200 mg). In all three species, the seed is a smooth and fusiform projectile and the spring is the endocarp, a hard structure that surrounds each seed (figure 1). As the endocarp desiccates, it deforms, applying forces on the seed [27]. However, the seed resists these forces, leading to energy storage of the endocarp. Ultimately, the forces keeping the seed in place are overcome by the forces applied by the endocarp. The seed is then squeezed out as the stored elastic potential energy in the endocarp propels the seed. In addition to their range of seed sizes,

Table 1. Elastic potential energy storage and release across the three Hamamelidaceae species. Values are reported as the mean and the standard deviation with the range in parentheses, except for the number of plants and the number of fruits.

species	*Loropetalum chinense*		*Hamamelis virginiana*		*Fortunearia sinensis*	
dataset	seed launch	seed reinsertion	seed launch	seed reinsertion	seed launch	seed reinsertion
number of plants	3	2	7	3	3	3
number of fruits	57	5	59	7	46	7
seed mass (mg)	29.18 ± 6.75 (13.95–43.89)	30.27 ± 2.91 (25.92–33.51)	56.38 ± 9.84 (26.36–78.02)	61.88 ± 8.47 (47.96–71.21)	137.79 ± 37.86 (52.40–205.66)	128.06 ± 21.61 (88.89–153.93)
endocarp mass (mg)	35.12 ± 9.40 (22.26–67.40)	35.68 ± 1.70 (33.06–37.25)	112.94 ± 20.40 (60.94–158.54)	127.14 ± 14.91 (101.35–148.70)	208.25 ± 34.37 (129.19–281.58)	196.23 ± 17.75 (178.36–231.09)
ratio (seed mass:endocarp mass)	0.84 ± 0.13 (0.53–1.31)	0.85 ± 0.10 (0.70–0.98)	0.50 ± 0.06 (0.29–0.66)	0.49 ± 0.03 (0.43–0.53)	0.65 ± 0.11 (0.32–0.80)	0.65 ± 0.08 (0.49–0.74)
launch speed (m s^{-1})	9.6 ± 1.0 (6.9–11.5)	9.3 ± 0.6 (8.6–10.1)	10.7 ± 1.3 (7.7–14.5)	10.8 ± 1.4 (7.9–12.6)	8.2 ± 1.7 (4.0–11.4)	9.5 ± 1.2 (7.5–10.5)
kinetic energy (mJ)	1.36 ± 0.38 (0.65–2.51)	1.30 ± 0.14 (1.18–1.53)	3.27 ± 1.00 (1.48–5.33)	3.72 ± 1.11 (1.48–4.75)	4.89 ± 2.16 (0.43–9.40)	5.74 ± 1.55 (3.64–8.00)
elastic potential energy (mJ)	n.a.	7.94 ± 2.89 (5.82–12.97)	n.a.	12.83 ± 7.37 (6.78–24.10)	n.a.	22.85 ± 4.78 (17.38–30.54)
mass-specific elastic potential energy (J kg^{-1})	n.a.	222 ± 84 (164–366)	n.a.	101 ± 50 (51–183)	n.a.	116 ± 24 (91–154)

the three witch hazel species share this mechanism by which one spring launches one seed, further facilitating the investigation of the mechanical relationship between the spring and seed.

Here we test how biological spring-actuated systems—exemplified by spring-propelled seeds—vary elastic potential energy storage across a range of projectile speeds and masses. We address three guiding questions related to scaling and trade-offs among elastic potential energy storage, projectile mass and projectile velocity across three seed-shooting Hamamelidaceae species: (i) How does elastic potential energy storage vary across species? (ii) How is the tradeoff between projectile speed and mass expressed given constant or varying elastic potential energy? (iii) How does variation in elastic potential energy storage occur through variation of spring morphology, specifically via spring size (measured in terms of mass)? Answers to these questions offer insights into how plants and other organisms navigate physical principles through coordinated variation of the spring and projectile across developmental and evolutionary timescales.

2. Methods

2.1. Study system

Loropetalum chinense, *Hamamelis virginiana* and *Fortunearia sinensis* are in the family Hamamelidaceae and are considered to be understory shrubs. A DNA sequence-based phylogeny placed these three species in the Hamamelidoideae subfamily, which is characterized by seed-shooting fruits [26]. Each species represents one of the three major clades of the Hamamelidoideae subfamily (figure 1).

Fruits were collected throughout the 2019, 2020 and 2021 witch hazel seed launch seasons (September–November) starting when at least one fruit on the plant showed signs of dehiscence. *Fortunearia sinensis* and *Loropetalum chinense* fruits were collected with permission from Duke Gardens, Durham, North Carolina, USA. *Hamamelis virginiana* fruits were collected from Duke Forest, Durham, North Carolina, USA under research permit R2122-522. Sample sizes are reported in table 1.

2.2. Measuring seed launch and its predictors

Seed launch kinematics were collected using high-speed videography (100 000 frames s^{-1}; 256 × 128 pixel resolution, 2.33 µs shutter speed; SA-Z, Photron, San Diego, CA, USA). For each test, we attached the intact fruit to a metal block by applying cyanoacrylate glue to the base of the fruit. The metal block was then clamped in place. By applying glue to the surface of the fruit and not the endocarp inside of the fruit, we ensured that the endocarp was free to recoil.

The seed was tracked throughout the initial frames of movement (auto-tracking MATLAB script; DLTdv8 MATLAB script; MATLAB 9.9, version R2020b [29]). The auto-tracking script placed a point on the leading tip of the seed for each frame, starting 10 frames before the seed starts to move and ending 50 frames after. The distance travelled by the seeds was calibrated with measurements of a millimetre-scale ruler filmed in the plane of focus after each seed launch. We used a stage micrometer (KR-814 stage micrometer, Klarmann Rulings, Inc., Litchfield, NH, USA) with a resolution of 0.02 mm to re-calibrate our ruler to 0.1 mm. The position data were then exported into R to calculate the maximum initial speed (v.3.6.1; R Foundation for Statistical Computing, https://www.r-project.org/). The maximum initial speed was calculated by finding the maximum value of the first derivative of position over the 60 frames.

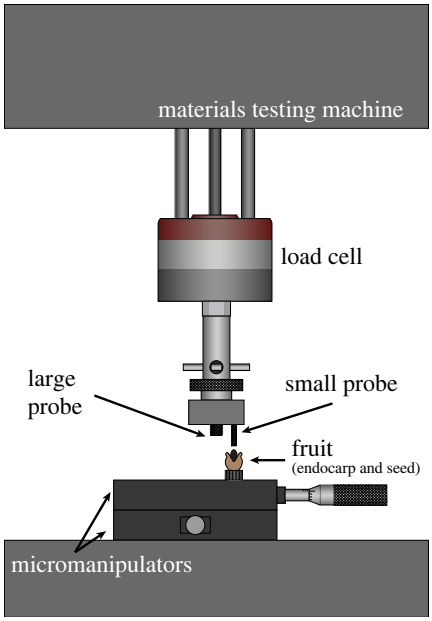

Figure 2. A materials testing machine was used to measure the force and displacement required to reinsert the seed into the endocarp. After the fruit launched its seed, we collected the seed and placed it loosely in the endocarp. The fruit, containing the endocarp and seed, was attached to a bolt head with cyanoacrylate glue. Two micromanipulators allowed for fine adjustment of the bolt, endocarp and seed assembly in two dimensions. The assembly was positioned underneath a set screw probe. An M3 set screw was used as the probe for testing *L. chinense* and *H. virginiana* while a larger M8 set screw was used as the probe for *F. sinensis*. The materials testing machine brought the probe down and recorded the distance travelled. A load cell measured the force required to reinsert the seed into the endocarp.

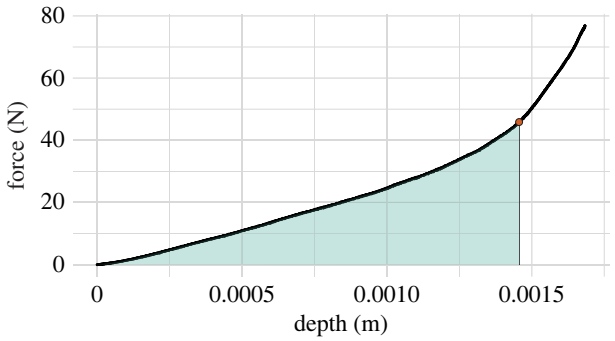

Figure 3. As the materials testing machine pressed a seed into an endocarp, two distinct slopes were evident and were separated by an inflection point. A piecewise function identified the inflection point (red circle). Before this point, the seed was deforming the endocarp walls as it was pushed deeper into the endocarp. Beyond this point, the seed began to push against the base of the endocarp, compressing the endocarp and the rest of the fruit (signified by a greater slope after the point). The work required to reinsert the seed (green fill) was calculated from the origin to the inflection point.

Once the fruit launched its seeds, we collected the seeds, ran materials tests on the fruit (see next section), extracted the endocarps from the fruit, and used a microbalance (0.001 mg readability, XPE56, Mettler Toledo, Columbus, OH, USA) to measure the mass of the seeds and endocarps. We calculated the ratio of seed mass to endocarp mass.

We calculated the kinetic energy of the launched seed as a function of the seed's mass and launch speed. Specifically, we used the equation $1/2 m_{seed} s_{seed}^2$ where m_{seed} is the mass of the seed and s_{seed} is the maximum initial speed of the seed. While we observed cracks on the endocarp prior to launch, these cracks formed well before seed launch and thus would not affect energetic measurements. This observation is corroborated by a study on *Hamamelis mollis* which also noted crack formation prior to launch and concluded that these cracks were not the unlatching mode [27].

We conducted an uncertainty analysis for speed and kinetic energy [30]. The analysis resulted in an uncertainty of 2% for speed (temporal resolution of 1×10^{-5} s, calibrated ruler resolution of 2×10^{-5} m) and 2% for kinetic energy (balance resolution of 1×10^{-9} kg).

2.3. Measuring elastic potential energy storage of the endocarp

To investigate the role of the endocarp in the energetic tradeoff between seed mass and launch speed, we first developed and validated a method for measuring elastic potential energy storage in the endocarp. Next, we used this method to measure how elastic potential energy storage varied across the endocarps of the three species. Finally, we measured how elastic potential energy scaled with endocarp mass.

We accounted for the complexities of the endocarp as a spring by performing materials tests on the entire structure [30,31]. We based our methods on a study that measured the elastic potential energy storage of similarly complex mantis shrimp springs. In this study, the mantis shrimp's entire raptorial appendage, containing the spring, was deformed with care to match the natural deformation range of the appendage [20]. We devised a similar method whereby the entire endocarp was deformed in a manner that closely resembled the endocarp's natural deformation prior to seed launch.

To estimate the elastic potential energy stored in the deformation of the endocarp, we used a materials testing machine (ElectroPuls E1000 outfitted with Instron Dynacell Dynamic Load Cell ± 250 N, catalogue no. 2527-131, Instron, Norwood, MA, USA) to reinsert the seed back into endocarp after it was launched (figure 2). We measured the force and displacement required to push the seed back into its original position and thereby calculated an estimate of the elastic potential energy stored through deformation of the endocarp. Displacement is defined as the depth at which the seed is pushed into the endocarp and, thus, we refer to this displacement as depth throughout the paper.

To push the seed back into the endocarp, we created a seed-pushing probe. The probe consisted of a set screw threaded into a metal block that was attached to the arm of the materials testing machine. The socket head of the set screw guided the seed during the tests. A small set screw (metric size M3) was used for testing *H. virginiana* and *L. chinense* fruits and a larger set screw (metric size M8) was used for testing *F. sinensis* fruits to accommodate for the wider seeds of *F. sinensis*. These design considerations prevented the seed from slipping out of the endocarp during the test while still allowing the seed to rotate as it does during launch.

The fruits were carefully positioned underneath the probe prior to a test. Immediately after seed launch, we affixed the fruit, still containing the endocarp, to a platform with cyanoacrylate glue. The seed was then loosely placed back into the endocarp cavity with care to match the natural orientation of the seed in the endocarp. We then used micromanipulators on the platform to position the fruit, now containing the endocarp and seed, directly beneath the seed-pushing probe (figure 2).

To conduct a test, the probe was lowered onto the seed, thereby pushing it into the endocarp. The seed was pushed into the endocarp at a rate of 0.1 mm s^{-1} until the seed was at the same depth in the endocarp as it was before it was launched

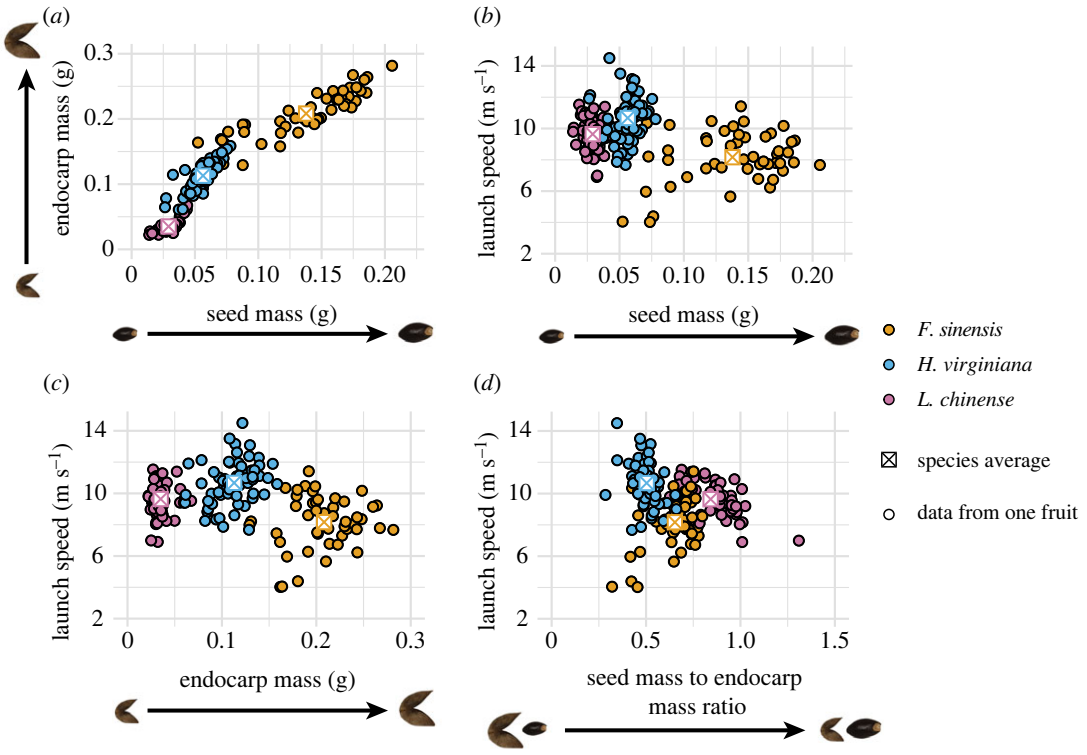

Figure 4. Endocarp mass increased with seed mass across and within species; however, seed launch speed was not associated with any of the mass measurements. (*a*) As seed mass increased, endocarp mass increased both within and across species. The proportional increase in endocarp mass relative to seed mass varied across the three species. (*b*) Across an order of magnitude increase in seed mass, average seed launch speed for the three species did not substantially decrease. It was notable that *F. sinensis* had the largest variance in seed masses. (*c*) Seed launch speed was also not associated with endocarp mass. *H. virginiana*, with intermediate endocarp masses, had the highest seed launch speeds. (*d*) The ratio of seed mass to endocarp mass was also not associated with seed launch speed.

(electronic supplementary material, figure S1 and table S1). The materials testing machine recorded the force and depth of the seed in the endocarp over time. See table 1 for sample sizes.

We analysed the force and depth data in terms of work (N m; J) and slope (N m^{-1}). To calculate the slopes, we used a piecewise linear regression. Specifically, we used the 'segmented' R package [32] to assign one to two breakpoints to each plot where the slope changed significantly. A slope was calculated for each of the sections of the plot created by the breakpoints (electronic supplementary material, figure S1). To calculate work (area under the force–depth curve for each of these sections; figure 3), we used the 'bayestestR' R package [33]. The code used to analyse these data are archived in Dryad: https://doi.org/10.5061/dryad.c59zw3rbn.

To ensure that we measured the slope that corresponded to when the seed was loading the endocarp rather than the slope when the endocarp was pushing into the experimental set-up, we performed a series of validation tests. Immediately following the seed reinsertion tests, we detached the fruit from the platform, removed the seed, and attached it to a custom-built clamp that grabbed onto the fruit. This clamp replaced the probe from the seed reinsertion tests. With this set-up, the fruit was pressed into the platform at a rate of 0.1 mm s^{-1} while the force output and depth of the fruit were recorded. The data were analysed in the same way as the seed reinsertion tests and the slopes from these validation experiments were compared to slopes from the seed reinsertion tests with a series of Welch's *t*-tests (electronic supplementary material, table S1).

Finally, having established a method to compare variation in elastic potential energy storage across the endocarps of the three species, we selected a scaling metric that related the morphology of the endocarp to its ability to store elastic potential energy. Given that our method relies on measuring deformations across the entire endocarp, the most encompassing morphological correlate with elastic potential energy storage is mass.

3. Results

3.1. Measuring seed launch and its predictors

Within and across species, endocarp mass increased as seed mass increased. The rate at which endocarp mass increased with seed mass differed across species, such that the relationship between seed mass and endocarp mass across species is nonlinear (figure 4*a*). The slope results are as follows—ranked from highest to lowest rate of endocarp mass increase for a given increase in seed mass: *H. virginiana* (slope = 1.691, Adjusted $R^2 = 0.6616$, *F*-statistic = 143.7, *p*-value: $< 1.0 \times 10^{-10}$), *L. chinense* (slope = 1.131, Adjusted $R^2 = 0.6530$, *F*-statistic = 112, *p*-value: $< 1.0 \times 10^{-10}$), then *F. sinensis* (slope = 0.7973, Adjusted $R^2 = 0.7664$, *F*-statistic = 158.5, *p*-value: $< 1.0 \times 10^{-10}$). The slopes from the three species cannot be compared statistically since there were not enough species included in our analysis to perform phylogeny-corrected statistics.

Seed mass and endocarp mass each spanned an order of magnitude across the three species (table 1), but seed launch speed was not associated with seed mass or endocarp mass (figure 4*b*,*c*). Within and across species, launch speed did not decrease as seed mass increased (figure 4*b*). However, species with larger average seed or endocarp masses had a greater variance of mass.

Within and across species, the ratio of seed mass to endocarp mass was not associated with seed launch speed (figure 4*d*). *Loropetalum chinense* fruits had the highest average seed mass to endocarp mass ratio, followed by *F. sinensis* fruits, then *H. virginiana* fruits (table 1). Across species, average seed launch speed was lowest for *F. sinensis* which exhibited an intermediate average seed mass to endocarp mass ratio.

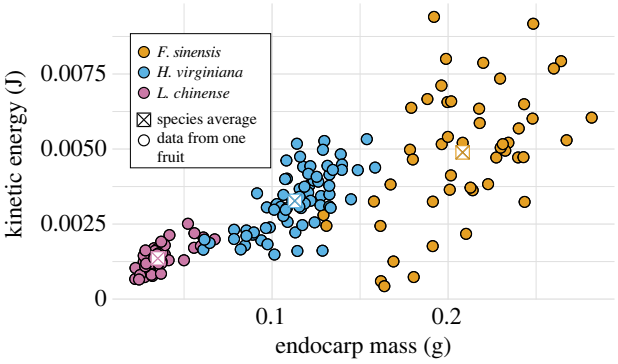

Figure 5. Across and within species, as endocarp mass increased, the kinetic energy of the seed also increased.

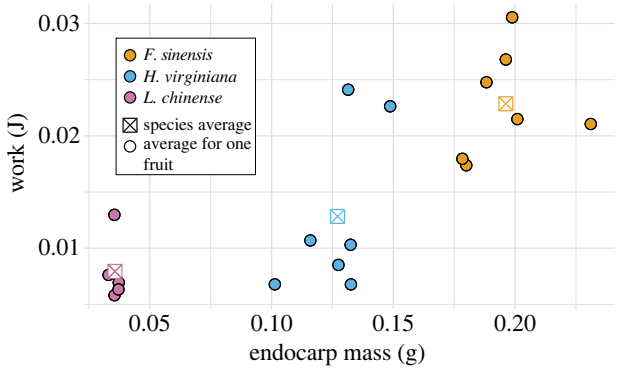

Figure 6. Across species, as endocarp mass increased, the work to reinsert the seed (elastic potential energy of the endocarp) increased.

Across and within species, seed kinetic energy increased with endocarp mass (figure 5). The rate at which seed kinetic energy increased with endocarp mass was highest in *H. virginiana* (Slope = 0.0338 J g^{-1}, Adjusted $R^2 = 0.4688$, F-statistic = 65.42, p-value = 1.049×10^{-11}) followed by *F. sinensis* (Slope = 0.0327 J g^{-1}, Adjusted $R^2 = 0.2552$, F-statistic = 17.45, p-value = 0.0001), then *L. chinense* (Slope = 0.0288 J g^{-1}, Adjusted $R^2 = 0.4896$, F-statistic = 57.59, p-value = 3.000×10^{-10}). Again, a phylogeny-corrected statistic comparing the slopes would require more than three species.

3.2. Measuring elastic potential energy storage of the endocarp

The seed reinsertion methods successfully differentiated between the seed deforming the endocarp walls and the seed pushing against the base of the endocarp and platform. We observed a change in slopes in the majority of the resulting plots. We used the piecewise regression to assign an inflection point to each plot that marked the change in slopes and broke the plot into two sections (electronic supplementary material, figure S1). The slopes for the second section of the seed reinsertion test plots were more similar to the slopes from the validation test plots compared to the first sections, indicated by Welch's t-tests (electronic supplementary material, table S1).

Across the three species, as endocarp mass increased, the work to deform the endocarp increased (figure 6, table 1). We defined work as the area under the curve calculated for the section of the seed reinsertion tests during which the seed deformed the endocarp walls. Meanwhile, mass-specific work was highest in the species with the smallest endocarp mass (*L. chinense*; figure 7*a*, table 1) and as seed mass to endocarp mass ratio increased, mass-specific work increased (figure 7*b*).

Work (i.e. elastic potential energy stored in the endocarp) was greater than the kinetic energy of seed launch for all fruits. When kinetic energy was plotted against potential energy, smaller fruits (less massive springs and seeds) were closer to a one-to-one line delineating a perfect conversion of elastic potential energy to kinetic energy compared with larger fruits (figure 8).

4. Discussion

Despite considerable variation in mass, the seeds of three witch hazel species were launched at similar speeds. We revealed differences in energetics resulting from diverse combinations of seed and spring masses. In summary, fruits that shot more massive seeds also had more massive springs that stored more elastic potential energy than smaller springs. The ratio of seed mass to endocarp mass varied across the three species. Fruits that shot larger seeds relative to their springs had more energy-dense springs, meaning that they stored more energy per mass. Finally, as fruit mass (seed mass plus endocarp mass) increased, energy conversion efficiency decreased.

We begin the discussion by sequentially examining key components of the ballistic equation—projectile launch speed, mass and kinetic energy [34,35]. We then examine these findings in the context of the latch-mediated spring actuation framework which focuses on how energy is stored in the spring and transferred into the projectile [30]. We conclude by critically examining emerging questions related to the evolution and operation of energy sources, springs and latches as integrated components.

4.1. Applying a ballistics framework: projectile mass and launch speed

Projectile launch speed, mass and kinetic energy define the energetics and kinematics of any ballistic system. Given the same kinetic energy at takeoff, as seed mass increases, launch speed should decrease. However, this relationship was not found across the three witch hazel species. Comparisons of previously studied seed-shooting plants provide additional examples of similar seed launch speeds despite a range of seed masses. The mean seed launch speed for *Vicia sativa* and *Croton capitatus* is 4.64 m s^{-1} and 4.71 m s^{-1}, respectively [36]. Yet, *V. sativa* seeds have a mean mass that is almost twice that of *C. capitatus* (23.3 mg compared to 12.8 mg [36]). Even more remarkable is the comparison between *Impatiens glandulifera* and *Cardamine parviflora*. *I. glandulifera* has an average seed mass of 20.7 mg while that of *C. parviflora* is only 0.15 mg, yet the average launch speeds of *I. glandulifera* and *C. parviflora* are 6.19 m s^{-1} and 6.29 m s^{-1}, respectively [37,38]. Therefore, for many seed-shooting plants, conclusions about launch speed cannot be made with seed mass alone, given that kinetic energy at launch varies.

Even in ballistic animal systems, such as the spring-powered jumps of locusts, launch speed did not trade off with projectile mass. Juvenile locusts, spanning tens to thousands of milligrams in body mass, did not vary significantly in launch speed [18]. Adult locusts had higher launch speeds than juveniles, but also did not experience a large variance in

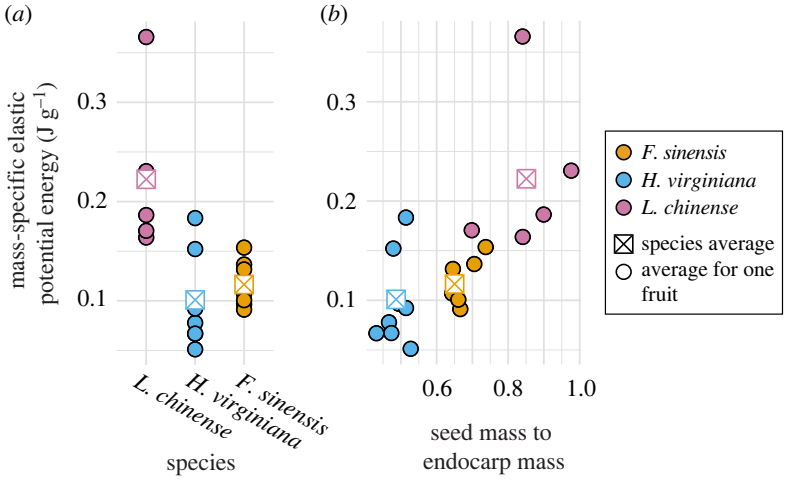

Figure 7. As the seed mass to endocarp mass ratio increased, mass-specific elastic potential energy increased. (*a*) Of the three species, *L. chinense* fruits had the highest mass-specific stored energy. (*b*) Fruits with smaller endocarps relative to their seeds stored more mass-specific elastic potential energy.

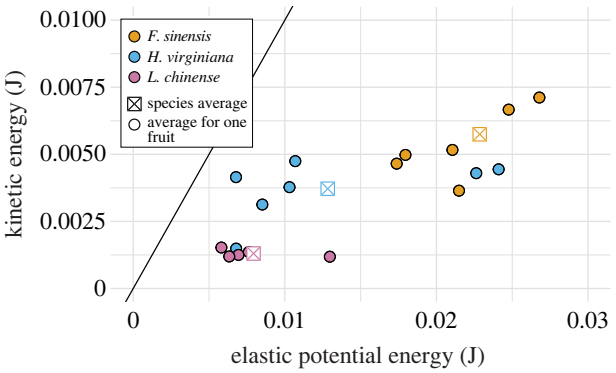

Figure 8. Of the three species, *L. chinense* had fruits with the most efficient conversion of elastic potential energy stored in the endocarp into kinetic energy of the seed. Some *H. virginiana* fruits were as efficient as *L. chinense* fruits, while *F. sinensis* fruits were the least efficient of the three. The black line denotes a perfect conversion of stored elastic potential energy into kinetic energy of the seed. Points in the region to the left of this line were impossible since they would imply that more energy was released than was stored. Points on the line were also impossible since some of the stored energy was lost to friction during seed launch.

launch speed across their range of body masses. Similar launch speeds within both the juvenile and adult groups were explained by differing uses of the jumps by each group [18]. Juveniles used jumps primarily for locomotion, such that consistent average launch speeds yielded a characteristic jump distance. Meanwhile, adults used jumps to reach the minimum launch speed off the ground needed to initiate flight. It was hypothesized that for both size groups, no significant benefit was achieved via higher launch speeds [18].

Similar launch speeds across an order of magnitude difference in Hamamelidaceae seed masses may be indicative of a threshold launch speed required to disperse seeds a certain distance. In the context of the ballistics equation and our earlier finding that kinetic energy at launch can increase, larger projectiles launched at similar speeds have more momentum and an increased dispersal distance. However, the spinning of seeds and other aerodynamic effects could cause the trajectory to diverge from this expectation [25,37,39]. While interesting, an investigation of aerodynamic effects was outside the realm of this study (see the electronic supplementary material for rotational kinetic energy measurements for spinning Hamamelidaceae seeds). Thus, future studies of drag and seed trajectories are required to relate our findings to dispersal distance [40].

To establish if dispersal distance drives variation in the elastic mechanism and energetics of these plants, two additional ballistics equation measurements are needed: the launch angle and starting height. For a given projectile and its drag profile, a theoretical launch angle maximizes distance [34,35]. Additionally, if all other parameters are held constant, fruits higher on the plant would be shot further [41]. Measurements of launch angle are particularly pertinent to witch hazel fruits given that the fruit's orientation is directly correlated with the launch angle of the seed due to the seed launching mechanism (witch hazel seeds are launched from one end of the fruit while for other seed-shooting mechanisms the fruit sends seeds in multiple directions [23,24,34,39,42]). Future investigations may reveal that fruit height is correlated with launch angle, seed mass and endocarp mass. Such findings would identify launch angle, seed mass and endocarp mass, as control parameters for the initial dispersal distance of the seed. Within-individual phenotypic plasticity across vertical gradients has been described in leaf and flower morphology [43].

4.2. Applying a latch-mediated spring actuation framework: the spring as the energy source

While the ballistic equation analyses projectile kinematics given the projectile's initial conditions such as its mass and launch speed, latch-mediated spring actuation considers the flow of energy from the spring to the projectile that results in the projectile's launch speed [30]. Relevant spring parameters include the total elastic potential energy stored in the spring, mass-specific elastic potential energy storage, ratio between seed and spring mass, and efficiency of converting elastic potential energy to kinetic energy. In the following two sections, we contextualize these measurements which are applicable to other seed-shooting systems as well as spring-actuated animal systems.

The endocarps of the three witch hazel species stored more energy on average than the springs of three other seed-shooting plants for which energy storage was measured experimentally. The fruits of *Impatiens capensis* [44], *Impatiens glandulifera* [42] and *Cardamine hirsuta* [24] generally use the

rapid coiling of springy strips of material, referred to as valves, to launch seeds. A combination of beam bending mechanics and measurements of the force required to uncoil the valves back to their pre-launch state from custom-built extensometers revealed that the springs of *I. capensis*, *I. glandulifera* and *C. hirsuta* stored 8, 0.9 and 0.5 mJ, respectively. In comparison, our study found that the endocarps of *L. chinense*, *H. virginiana* and *F. sinensis* stored 8, 13 and 23 mJ on average, respectively.

Endocarp mass was a good predictor of the endocarp's ability to store elastic potential energy. The constant launch speeds across seed masses can therefore be explained by fruits with larger seeds having larger springs. More importantly, the relationship between endocarp mass and its ability to store elastic potential energy allowed for the testing of an additional integrative metric: the ratio of seed mass to endocarp mass. Because launch speed remained constant across seed masses, fruits with larger seeds had greater kinetic energy. Meanwhile, since elastic potential energy storage increased with endocarp mass, fruits with larger endocarps had greater elastic potential energy storage. The ratio of seed to endocarp mass accounts for both of these effects on energetics.

The ratio of seed mass to endocarp mass contextualizes differences in the mass-specific elastic potential energy storage of endocarps. Each witch hazel species had a different average seed mass to endocarp mass ratio (figure 4*d*). For example, *L. chinense* had the least massive seeds of the three species (figure 4*b*), yet because it had proportionally smaller endocarps, it also had the most massive seeds relative to its endocarp mass (figure 4*d*). One explanation for the consistent launch speeds across ratios was that the springs of fruits with higher ratios were able to store more energy relative to their mass (figure 7*b*).

The mass-specific elastic potential energy storage in the three witch hazel species was within the range of previously studied mass-specific elastic potential energy storage of seed-shooting plant springs. Empirical measurements found that the mass-specific elastic potential energy storage of *Impatiens capensis* was 124 J kg^{-1} [44] while the mean mass-specific elastic potential energy storage of *Cardamine parviflora* was 89.3 J kg^{-1} [38]. In comparison, the range of mass-specific elastic potential energy storage was 100 J kg^{-1} to 200 J kg^{-1} across the three Hamamelidaceae species.

The relationship between seed mass and endocarp mass exemplified by the ratio of their masses suggests the potential for a resource investment tradeoff during the fruit's development. Resource-limited plants may face a tradeoff between investing resources into increasing the size of the seed or the size of the spring. This may result in various seed mass to endocarp mass ratios, launch speeds, and ultimately dispersal patterns. Alternatively, adjustments of the endocarp, such as increased mass-specific elastic potential energy storage, may allow for robustness in launch speeds across a range of seed to endocarp mass ratios as found in our study. However, to address this resource investment tradeoff, studies should test the consequences of resource limitation on the development of plant latch-mediated spring actuation mechanisms.

Finally, examining how energy storage increases with body mass in mantis shrimp provides insight into potential mechanisms for how energy storage increases with endocarp mass. Larger mantis shrimp can store more elastic potential energy not because their springs have higher spring constants but rather because they can deform them more [20]. Thus, the muscle's ability to load energy into the spring was identified as a potential limiting factor in these mantis shrimp. The scaling of endocarps in Hamamelidaceae may follow a similar pattern in which larger endocarps are deformed more than smaller ones rather than increasing in spring constant. Measuring where along the endocarp deformation occurs as well as the magnitude of deformation thus emerges as an interesting future direction.

4.3. Applying a latch-mediated spring actuation framework: energy conversion efficiency

Comparative studies of the springs of seed-shooting plants reveal that springs storing low amounts of energy can achieve a greater than expected kinetic energy by more efficiently converting stored elastic potential energy to kinetic energy. For example, *Impatiens glandulifera* and *Impatiens capensis* share a seed-shooting mechanism that uses the rapid coiling of a springy strip of material to launch seeds. The fruits of *I. glandulifera* launch a greater number of heavier seeds per fruit at greater speeds (5–10 seeds per fruit, mean mass of 19.9 mg, mean speed of 3 m s^{-1} [42]) than those of *I. capensis* (2–5 seeds per fruit, mean mass of 10.7 mg, mean speed of 1.24 m s^{-1} [44]). Experiments conducted on the entire springs of these plants found that despite the increased kinetic energy demand of the fruits of *I. glandulifera*, their springs stored less energy than those of *I. capensis* (around 1 mJ for *I. glandulifera* versus 8 mJ for *I. capensis*). However, due to differences in the shapes of the elastic strips between the two species, the fruits of *I. glandulifera* had an energy conversion efficiency close to 100% compared to an energy conversion efficiency of 50% for *I. capensis* [42,44]. Similarly, in our dataset, *L. chinense*, which launched the largest seeds relative to its endocarp mass, had springs with the most efficient conversion of elastic potential energy to kinetic energy. Meanwhile, *F. sinensis* stored the most elastic potential energy, yet was the least efficient energy converter resulting in both species having similar launch speeds.

Examining the other components involved in latch-mediated spring actuation can reveal additional methods of adjusting elastic potential energy storage and release. Besides the projectile and spring, other components of spring-actuated systems include the motor (which loads energy into the spring [45,46] and the latch (which mediates the transition of elastic potential energy to kinetic energy [30,47]). The tuning of muscles (the motor) to tendons (the spring) explains why some frog species had higher mass-specific elastic potential energy storage in their tendons than others [45]. The species that stored the most mass-specific elastic potential energy had the stiffest springs and was able to deform these springs with muscles that generated greater forces due to improved pennation angles compared to the other species [45]. In the three witch hazel species, the motor is hypothesized to be the desiccation of the endocarp [15,27]. Thus, the endocarp acts as a structurally integrated motor–spring system. Future investigations can uncover how witch hazel fruits adjust the endocarp to fulfil its roles as both a motor and a spring and how the endocarps of *L. chinense* were able to store more energy per mass compared with those of the other species. Such an investigation may also reveal that limitations of the motor in this system explain our observed relationship between seed mass and endocarp mass (figure 4*a*).

The morphology of the latch can alter the amount of energy dissipated during the conversion of elastic potential energy to kinetic energy of the projectile. For example, in the spring-actuated mandible strikes of Dracula ants (*Mystrium camillae*), the tips of their two mandibles push against each other until the latch mandible slips off the strike mandible, resulting in the rapid acceleration of the strike mandible in a motion similar to a finger snap [2]. Large worker ants had latch mandibles with greater radii resulting in more energy dissipated during the unlatching and a lower maximum strike velocity [47]. Similarly, in the witch hazels, latching dynamics may scale with fruit size, because friction between the endocarp and seed may be the latch [27,48]. A decrease in the surface area of contact between the seed and the endocarp may result in fewer losses for the smaller seeds of *L. chinense* than the larger seeds of *F. sinensis*. However, to fully understand the role of friction in seed launch, future experiments are required.

4.4. Comparisons to synthetic spring-actuated systems

For biological and synthetic spring-actuated systems, the maximum amount of elastic potential energy stored in the spring depends on how well the motor and spring are tuned to one another [13,45,49]. If the spring is too stiff, the motor cannot load the spring to its full potential. Likewise, if the motor's work output exceeds the spring's elastic potential energy storage capacity, the motor's output is underused. For many synthetic and animal systems, the motor and the spring are separate structures that must be tuned to one another to form an integrated unit [13]. Examples of motors for synthetic systems include shape memory alloy [50,51], rotary motors [52], pneumatic or hydraulic artificial muscles [53], or external magnetic fields [54]. These motors can be integrated with springs. While one might expect springs to be metal coils and sheets, they also include more complex geometry [50], materials such as rubbers or carbon fibre [49,52], and can exhibit dynamic loading and recoiling through the use of meta-materials [55]. Meanwhile, animals typically use muscles as motors and can vary pennation angle [45], cross sectional area, and sarcomere length [56] to adjust muscle outputs. Animal springs include tendons, apodemes, and exoskeletons and can vary greatly in morphology and material composition [30].

Unlike the previously described synthetic and animal systems, seed-shooting witch hazel species and other seed-shooting plants use a single structure as both a motor and a spring [23,24,42,44,57]. The motor is either the movement of water into the spring (building turgor pressure) or the movement of water out of the spring through evaporation [8,58]. Therefore, tuning the motor to the spring for these plant systems entails balancing a single structure's role as both a motor and a spring. For example, in the witch hazel endocarp, desiccation of the structure affects its roles as both a motor and spring. As a motor, the endocarp depends on desiccation to drive deformation. However, as a spring, the endocarp's stiffness increases as it desiccates, changing its ability to store energy as it deforms. Our study, along with studies measuring elastic potential energy storage in other seed-shooting plant springs, sets the foundation for understanding how plants balance the roles of these combined motor–spring structures. By investigating the endocarp as a spring, we found that while absolute elastic potential energy storage increased with endocarp mass, the species with the least massive endocarps stored the most mass-specific elastic potential energy. Future studies investigating the endocarp as a motor may reveal how the morphology of the endocarp also facilitates the accumulation of strain energy through water loss such as by increasing surface area or varying thickness [15]. Furthermore, morphological features may reflect trade-offs between the structure's function as a motor or as a spring.

Engineers have begun to explore the use of a single structure as both a motor and spring for synthetic spring actuation. A synthetic hydrogel jumper, inspired by the ultrafast buckling motions of plants, uses spring actuation to perform multiple jumps [59]. Like the seed-shooting witch hazel endocarps, this jumper is a single structure that is both a motor and a spring. The hemisphere shape of the jumper facilitates the asymmetric evaporation of a solvent, the energy source for the jumps. Increased rates of evaporation on the convex side relative to the concave side of the hemisphere cause an accumulation of strain energy that triggers an eversion of the hemisphere [59]. The hydrogel jumper is representative of the rich design space emerging through combined motor–spring structures.

Continued investigation of seed-shooting plants can inform the design of synthetic spring-actuated systems. Implicit in the use of combined motor–spring structures for spring actuation is a reduction of components compared to traditional systems which consist of a separate motor and spring. Furthermore, combining the motor and spring into one structure may facilitate the capturing of energy from the environment through processes like evaporation. The previously mentioned hydrogel jumper captured 15.6 J of energy from the environment to power its jumps [59]. Although the kinetic energy output was optimized for this material, less than 1% of the captured energy was converted into kinetic energy [59]. Nevertheless, this jumper reveals the potential for harnessing environmental energy to power actuation. Attempting the same kinetic energy output optimization for other materials may allow for greater use of the captured energy from evaporation. The witch hazel and other seed-shooting plants provide a wealth of examples of materials and geometries used to form combined motor–spring structures [8,21]. Measuring these biological systems using measurements shared with engineers, such as the energy captured from the environment, elastic potential energy stored in the spring, and kinetic energy, will hasten the translation of biological designs into synthetic innovation.

Ethics. This work did not require ethical approval from a human subject or animal welfare committee.

Data accessibility. The R code used to analyze the data and the raw data tables are available from the Dryad Digital Repository: https://doi.org/10.5061/dryad.c59zw3rbn [60].

The data are provided in electronic supplementary material [61].

Declaration of AI use. We have not used AI-assisted technologies in creating this article.

Authors' contributions. J.F.J.: conceptualization, data curation, formal analysis, investigation, methodology, project administration, software, supervision, validation, visualization, writing—original draft, writing—review and editing; S.N.P.: formal analysis, funding acquisition, project administration, resources, supervision, validation, writing—review and editing.

Conflict of interest declaration. We declare we have no competing interests.

Funding. This material is based on work supported by the US Army Research Laboratory and the US Army Research Office under contract/grant no. W911NF-15-1-0358 and the National Science Foundation Division of Integrative Organismal Biology under grant no. 2019323, both awarded to S.N.P.

Acknowledgements. We thank the Duke Gardens, especially Paul Jones and Kati Henderson, and Duke Forest, especially Sara Childs, for their help in the collection of fruits. We would also like to acknowledge Paul Manos, Tyson Hedrick, Kathleen Donohue, Sayan Mukherjee, the Patek Lab, and the Impulsive MURI team, especially Elayne Thomas, Al Crosby, and Nak-seung Patrick Hyun, for their feedback and support.

References

1. Burrows M, Shaw SR, Sutton GP. 2008 Resilin and chitinous cuticle form a composite structure for energy storage in jumping by froghopper insects. *BMC Biol.* **6**, 41. (doi:10.1186/1741-7007-6-41)
2. Larabee FJ, Smith AA, Suarez AV. 2018 Snap-jaw morphology is specialized for high-speed power amplification in the Dracula ant, *Mystrium camillae*. *R. Soc. Open Sci.* **5**, 181447. (doi:10.1098/rsos.181447)
3. Longo SJ, Ray W, Farley GM, Harrison J, Jorge J, Kaji T, Palmer AR, Patek SN. 2021 Snaps of a tiny amphipod push the boundary of ultrafast, repeatable movement. *Curr. Biol.* **31**, R116–R117. (doi:10.1016/j.cub.2020.12.025)
4. Nüchter T, Benoit M, Engel U, Özbek S, Holstein TW. 2006 Nanosecond-scale kinetics of nematocyst discharge. *Curr. Biol.* **16**, R316–R318. (doi:10.1016/j.cub.2006.03.089)
5. Patek SN. 2019 The power of mantis shrimp strikes: interdisciplinary impacts of an extreme cascade of energy release. *Integr. Comp. Biol.* **59**, 1573–1585. (doi:10.1093/icb/icz127)
6. Patek SN, Baio JE, Fisher BL, Suarez AV. 2006 Multifunctionality and mechanical origins: ballistic jaw propulsion in trap-jaw ants. *Proc. Natl Acad. Sci. USA* **103**, 12 787–12 792. (doi:10.1073/pnas.0604290103)
7. Pringle A, Patek SN, Fischer M, Stolze J, Money NP. 2005 The captured launch of a ballistospore. *Mycologia* **97**, 866–871. (doi:10.1080/15572536.2006.11832777)
8. Sakes A, van der Wiel M, Henselmans PWJ, van Leeuwen JL, Dodou D, Breedveld P. 2016 Shooting mechanisms in nature: a systematic review. *PLoS ONE* **11**, e0158277. (doi:10.1371/journal.pone.0158277)
9. Schulz JR, Jan I, Sangha G, Azizi E. 2019 The high speed radular prey strike of a fish-hunting cone snail. *Curr. Biol.* **29**, R788–R789. (doi:10.1016/j.cub.2019.07.034)
10. Seid MA, Scheffrahn RH, Niven JE. 2008 The rapid mandible strike of a termite soldier. *Curr. Biol.* **18**, R1049–R1050. (doi:10.1016/j.cub.2008.09.033)
11. Swaine MD, Beer T. 1977 Explosive seed dispersal in *Hura Crepitans L.* (Euphorbiaceae). *New Phytol.* **78**, 695–708. (doi:10.1111/j.1469-8137.1977.tb02174.x)
12. Singh AK, Prabhakar S, Sane SP. 2011 The biomechanics of fast prey capture in aquatic bladderworts. *Biol. Lett.* **7**, 547–550. (doi:10.1098/rsbl.2011.0057)
13. Ilton M *et al.* 2018 The principles of cascading power limits in small, fast biological and engineered systems. *Science* **360**, eaao1082. (doi:10.1126/science.aao1082)
14. Ilton M, Cox SM, Egelmeers T, Sutton GP, Patek SN, Crosby AJ. 2019 The effect of size-scale on the kinematics of elastic energy release. *Soft Matter* **15**, 9579–9586. (doi:10.1039/C9SM00870E)
15. Skotheim JM. 2005 Physical limits and design principles for plant and fungal movements. *Science* **308**, 1308–1310. (doi:10.1126/science.1107976)
16. Anderson PSL, LaCosse J, Pankow M. 2016 Point of impact: the effect of size and speed on puncture mechanics. *Interface Focus* **6**, 20150111. (doi:10.1098/rsfs.2015.0111)
17. Burrows M. 1995 Motor patterns during kicking movements in the locust. *J. Comp. Physiol. A* **176**, 289–305. (doi:10.1007/BF00219055)
18. Katz SL, Gosline JM. 1993 Ontogenetic scaling of jump performance in the African desert locust (*Schistocerca gregaria*). *J. Exp. Biol.* **177**, 81–111. (doi:10.1242/jeb.177.1.81)
19. McGowan CP. 2005 The mechanics of jumping versus steady hopping in yellow-footed rock wallabies. *J. Exp. Biol.* **208**, 2741–2751. (doi:10.1242/jeb.01702)
20. Zack TI, Claverie T, Patek SN. 2009 Elastic energy storage in the mantis shrimp's fast predatory strike. *J. Exp. Biol.* **212**, 4002–4009. (doi:10.1242/jeb.034801)
21. Ridley HN. 1930 *The dispersal of plants throughout the world*. Ashford, UK: L. Reeve & Company.
22. Lorts CM, Briggeman T, Sang T. 2008 Evolution of fruit types and seed dispersal: a phylogenetic and ecological snapshot. *J. System. Evol.* **46**, 396–404. (https://www.jse.ac.cn/EN/10.3724/SP.J.1002.2008.08039)
23. Li S, Zhang Y, Liu J. 2020 Seed ejection mechanism in an Oxalis species. *Sci. Rep.* **10**, 8855. (doi:10.1038/s41598-020-65885-2)
24. Hofhuis H *et al.* 2016 Morphomechanical innovation drives explosive seed dispersal. *Cell* **166**, 222–233. (doi:10.1016/j.cell.2016.05.002)
25. Ribera J, Desai A, Whitaker DL. 2020 Putting a new spin on the flight of jabillo seeds. *Integr. Comp. Biol.* **60**, 919–924. (doi:10.1093/icb/icaa117)
26. Li J, Bogle AL, Klein AS. 1999 Phylogenetic relationships of the Hamamelidaceae inferred from sequences of internal transcribed spacers (ITS) of nuclear ribosomal DNA. *Am. J. Bot.* **86**, 1027–1037. (doi:10.2307/2656620)
27. Poppinga S, Böse A-S, Seidel R, Hesse L, Leupold J, Caliaro S, Speck T. 2019 A seed flying like a bullet: ballistic seed dispersal in Chinese witch-hazel (*Hamamelis mollis* OLIV., Hamamelidaceae). *J. R. Soc. Interface* **16**, 20190327. (doi:10.1098/rsif.2019.0327)
28. Tiffney BH. 1986 Fruit and seed dispersal and the evolution of the Hamamelidae. *Ann. Missouri Bot. Garden* **73**, 394–416. (doi:10.2307/2399119)
29. Hedrick TL. 2008 Software techniques for two- and three-dimensional kinematic measurements of biological and biomimetic systems. *Bioinspir. Biomim.* **3**, 034001. (doi:10.1088/1748-3182/3/3/034001)
30. Longo SJ, Cox SM, Azizi E, Ilton M, Olberding JP, St Pierre R, Patek SN. 2019 Beyond power amplification: latch-mediated spring actuation is an emerging framework for the study of diverse elastic systems. *J. Exp. Biol.* **222**, jeb197889. (doi:10.1242/jeb.197889)
31. Rosario MV, Patek SN. 2015 Multilevel analysis of elastic morphology: the mantis shrimp's spring. *J. Morphol.* **276**, 1123–1135. (doi:10.1002/jmor.20398)
32. Muggeo VMR. 2017 Interval estimation for the breakpoint in segmented regression: a smoothed score-based approach. *Aust. N. Z. J. Stat.* **59**, 311–322. (doi:10.1111/anzs.12200)
33. Makowski D, Ben-Shachar M, Lüdecke D. 2019 bayestestR: describing effects and their uncertainty, existence and significance within the Bayesian framework. *JOSS* **4**, 1–8. (doi:10.21105/joss.01541)
34. Beer T, Swaine MD. 1977 On the theory of explosively dispersed seeds. *New Phytol.* **78**, 681–694. (doi:10.1111/j.1469-8137.1977.tb02173.x)
35. Vogel S. 2005 Living in a physical world II. The bio-ballistics of small projectiles. *J. Biosci.* **30**, 167–175. (doi:10.1007/BF02703696)
36. Garrison WJ, Miller GL, Raspet R. 2000 Ballistic seed projection in two herbaceous species. *Amer. J. Bot.* **87**, 1257–1264. (doi:10.2307/2656718)
37. Chapman DS, Gray A. 2012 Complex interactions between the wind and ballistic seed dispersal in *Impatiens glandulifera* (Royle). *J. Ecol.* **100**, 874–883. (doi:10.1111/j.1365-2745.2012.01977.x)
38. Hayashi M, Gerry SP, Ellerby DJ. 2010 The seed dispersal catapult of *Cardamine parviflora* (Brassicaceae) is efficient but unreliable. *Amer. J. Bot.* **97**, 1595–1601. (doi:10.3732/ajb.1000173)
39. Cooper ES, Mosher MA, Cross CM, Whitaker DL. 2018 Gyroscopic stabilization minimizes drag on *Ruellia ciliatiflora* seeds. *J. R. Soc. Interface* **15**, 20170901. (doi:10.1098/rsif.2017.0901)
40. Vogel S. 2009 *Glimpses of creatures in their physical worlds*. Princeton, NJ: Princeton University Press.
41. Thomson FJ, Moles AT, Auld TD, Kingsford RT. 2011 Seed dispersal distance is more strongly correlated with plant height than with seed mass: dispersal distance and seed mass. *J. Ecol.* **99**, 1299–1307. (doi:10.1111/j.1365-2745.2011.01867.x)

42. Deegan RD. 2012 Finessing the fracture energy barrier in ballistic seed dispersal. *Proc. Natl Acad. Sci. USA* **109**, 5166–5169. (doi:10.1073/pnas.1119737109)
43. Herrera CM. 2009 *Multiplicity in unity: plant subindividual variation and interactions with animals*. Chicago, IL: University of Chicago Press.
44. Hayashi M, Feilich KL, Ellerby DJ. 2009 The mechanics of explosive seed dispersal in orange jewelweed (*Impatiens capensis*). *J. Exp. Bot.* **60**, 2045–2053. (doi:10.1093/jxb/erp070)
45. Mendoza E, Azizi E. 2021 Tuned muscle and spring properties increase elastic energy storage. *J. Exp. Biol.* **224**, jeb243180. (doi:10.1242/jeb.243180)
46. Rosario MV, Sutton GP, Patek SN, Sawicki GS. 2016 Muscle–spring dynamics in time-limited, elastic movements. *Proc. R. Soc. B* **283**, 20161561. (doi:10.1098/rspb.2016.1561)
47. Divi S, Ma X, Ilton M, St. Pierre R, Eslami B, Patek SN, Bergbreiter S. 2020 Latch-based control of energy output in spring actuated systems. *J. R. Soc. Interface* **17**, 20200070. (doi:10.1098/rsif.2020.0070)
48. Li G *et al.* 2023 Biomimetic 4D printing catapult: from biological prototype to practical implementation. *Adv. Funct. Mater.* **33**, 2301286. (doi:10.1002/adfm.202301286)
49. Haldane DW, Plecnik MM, Yim JK, Fearing RS. 2016 Robotic vertical jumping agility via series-elastic power modulation. *Sci. Robot.* **1**, eaag2048. (doi:10.1126/scirobotics.aag2048)
50. Kim S-W, Koh J-S, Lee J-G, Ryu J, Cho M, Cho K-J. 2014 Flytrap-inspired robot using structurally integrated actuation based on bistability and a developable surface. *Bioinspir. Biomim.* **9**, 036004. (doi:10.1088/1748-3182/9/3/036004)
51. Zhakypov Z, Mori K, Hosoda K, Paik J. 2019 Designing minimal and scalable insect-inspired multi-locomotion millirobots. *Nature* **571**, 381–386. (doi:10.1038/s41586-019-1388-8)
52. Hawkes EW, Xiao C, Peloquin R-A, Keeley C, Begley MR, Pope MT, Niemeyer G. 2022 Engineered jumpers overcome biological limits via work multiplication. *Nature* **604**, 657–661. (doi:10.1038/s41586-022-04606-3)
53. Niiyama R, Nagakubo A, Kuniyoshi Y. 2007 Mowgli: a bipedal jumping and landing robot with an artificial musculoskeletal system. In *Proc. 2007 IEEE Int. Conf. on Robotics and Automation, Rome, Italy, 10–14 April 2007*, pp. 2546–2551. (doi:10.1109/ROBOT.2007.363848)
54. Mao G, Schiller D, Danninger D, Hailegnaw B, Hartmann F, Stockinger T, Drack M, Arnold N, Kaltenbrunner M. 2022 Ultrafast small-scale soft electromagnetic robots. *Nat. Commun.* **13**, 4456. (doi:10.1038/s41467-022-32123-4)
55. Liang X, Fu H, Crosby AJ. 2022 Phase-transforming metamaterial with magnetic interactions. *Proc. Natl Acad. Sci. USA* **119**, e2118161119. (doi:10.1073/pnas.2118161119)
56. Gronenberg W, Paul J, Just S, Hölldobler B. 1997 Mandible muscle fibers in ants: fast or powerful? *Cell Tissue Res.* **289**, 347–361. (doi:10.1007/s004410050882)
57. Evangelista D, Hotton S, Dumais J. 2011 The mechanics of explosive dispersal and self-burial in the seeds of the filaree, *Erodium cicutarium* (Geraniaceae). *J. Exp. Biol.* **214**, 521–529. (doi:10.1242/jeb.050567)
58. Edwards J, Laskowski M, Baskin TI, Mitchell N, DeMeo B. 2019 The role of water in fast plant movements. *Integr. Comp. Biol.* **59**, 1525–1534. (doi:10.1093/icb/icz081)
59. Kim Y, van den Berg J, Crosby AJ. 2021 Autonomous snapping and jumping polymer gels. *Nat. Mater.* **20**, 1695–1701. (doi:10.1038/s41563-020-00909-w)
60. Jorge JF, Patek SN. 2023 Data from: Elastic pinch biomechanisms can yield consistent launch speeds regardless of projectile mass. Dryad Digital Repository. (doi:10.5061/dryad.c59zw3rbn)
61. Jorge JF, Patek SN. 2023 Elastic pinch biomechanisms can yield consistent launch speeds regardless of projectile mass. Figshare. (doi:10.6084/m9.figshare.c.6777699)